

Studies on Performances of Copper Oxide Nanoparticles from *Catharanthus Roseus* Leaf Extract



K. A. Khan, M. Shaiful Islam, Md. Abdul Awal, M. N. Islam Khan, and A. K. M. Atique Ullah

1 Introduction

The CuO Nanoparticles from *Catharanthus Roseus* leaf extract is an innovative idea [1–4]. Although it has been conducted MnO₂ NPs from *Bryophillim pinnatum* leaf extract by our research group previously [5–10] It has been conducted the different characterizations like XRD, GC–MS, SEM, FESEM, FTIR, EDX, DSC, VSM, TGA, etc. The CuO nanoparticles are stable, robust, and have a longer shelf life compared to organic, antimicrobial agents [11–13]. There are a few strategies for the union of CuO NPs, which incorporate sol–gel process, co-precipitation, sonochemical method, hydrothermal techniques, non-aqueous synthesis, ultrasound irradiation, micro-emulsion method, electrochemical and microwave irradiation synthetic route, and so on [14–16]. The main aim of our research work on CuO Nanoparticles (NPs) is to use for electricity generation system by using electrochemical cell. The *Catharanthus Roseus* leaf is also a medicinal leaf [17–21]. It has a great medicinal value. There are some countries where it is used as a medicinal value. The biogenic amalgamation includes the blend of NPs utilizing plants and microorganisms or their concentrates [22, 23]. The microbial combination is a tedious and to some degree dangerous strategy, since it includes the upkeep of microbial societies under advanced, septic research center conditions. Developing a facile and green method for synthesizing

K. A. Khan (✉) · M. Shaiful Islam
Department of Physics, Jagannath University, Dhaka 1100, Bangladesh

Md. A. Awal
Department of Chemistry, National University, Gazipur, Bangladesh

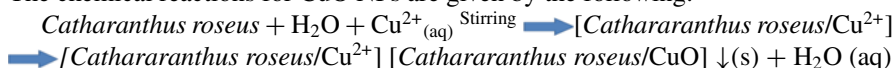
M. N. I. Khan
Nanoscience and Technology Research Laboratory, Atomic Energy Centre, Atomic Energy Commission, Dhaka 1000, Bangladesh

A. K. M. A. Ullah
Nanoscience and Technology Research Laboratory, Chemistry Division, Atomic Energy Centre, Bangladesh Atomic Energy Commission, Dhaka 1000, Bangladesh

CuO Nanoparticles (NPs) is of importance and still a challenge for materials scientists [24, 25]. The *Catharanthus roseus* leaves possess biomolecules such as terpenoid, carotenoid, sterol, alcohol, and organic acid, which could be used as reducing agent to react with Cu^{2+} ions as scaffolds to direct the formation of the CuO Nanoparticles (NPs) in a solution that have been extensively explored for possible medical applications [26]. The CuO Nanoparticles (NPs) from *Catharanthus roseus* leaves provide a particularly useful platform and demonstrate unique properties with potentially wide-ranging therapeutic applications [27].

2 Methodology

CuO NPs were synthesized via a facile green synthesis route where $(\text{Cu}(\text{CH}_3\text{COO})_2 \cdot \text{H}_2\text{O})$ were used as a precursor and *Catharanthus roseus* leaf extract was used as a source of reducing and capping agents. To synthesis CuO NPs, the *Catharanthus roseus* leaf extract was added to an aqueous mixture of Cu^{2+} acetate at a 1:1 M ratio. The chemical reactions for CuO NPs are given by the following:



The method of *Catharanthus Roseus* leaf extract preparation for getting CuO Nanoparticles (NPs) is shown in Fig. 1. From Fig. 1, it is found that the finished product was *Catharanthus Roseus* leaf extract (C.R.L. extract).

The method of CuO Nanoparticles (NPs) preparation using *Catharanthus Roseus* leaf extract is shown in Fig. 2. Finally, it is found (from Fig. 2) that the finished product was CuO Nanoparticles (NPs) using *Catharanthus Roseus* leaf extract (C.R.L. extract).

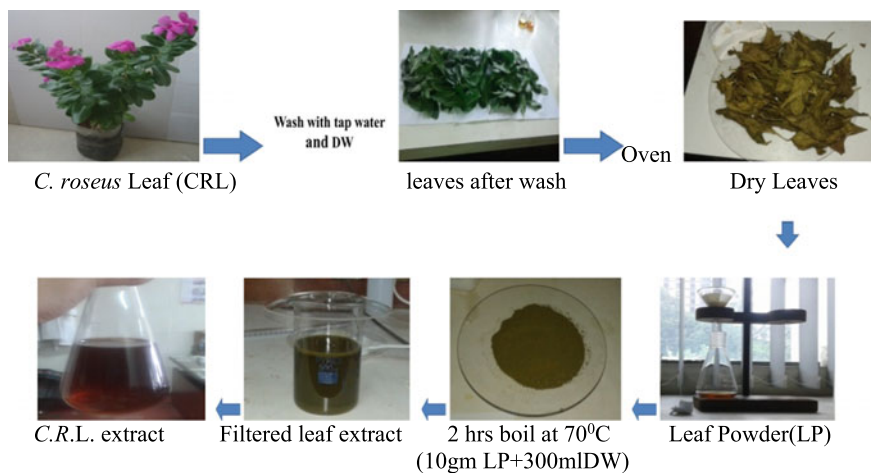


Fig. 1 Method of leaf extracts preparation

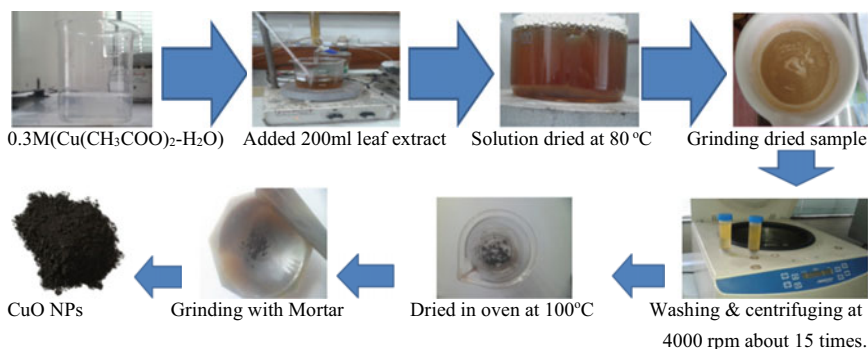


Fig. 2 Methods for sample preparation of CuO NPs

3 Results and Discussion

Table 1 shows the amount inpercentage (%) of functional group of *Catharanthus roseus* leaf extracts. It is found that the maximum functional group present in *Catharanthus roseus* leaf extract was Alcohol (42.64%) and the minimum functional group present in *Catharanthus roseus* leaf extract was Carotenoid (1.82%).

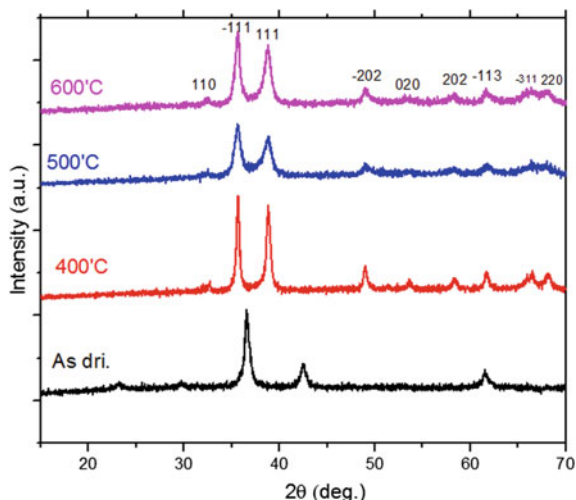
3.1 Structural Analysis Using XRD

It is shown (in Fig. 3) that the diffraction peaks of synthesized CuO NPs are assigned to the crystal planes of (110), (-111), (111); (-202), (020), (202); (-113), (-311), and (220), respectively. The analyzed diffraction peaks were matched well with the standard magnetite XRD patterns with JCPDS file no: 05-0661, which declared the crystallographic system of the monoclinic structure.

Table 1 Functional group present in *Catharanthus roseus* leaf extracts

Functional group	Amount (%)
Alcohol	42.64
sterol	23.03
Alkane	3.43
Ketone	10.14
Terpenoid	2.67
Carboxylic acid	2.43
Carotenoid	1.82

Fig. 3 XRD patterns of CuO Nanoparticles



3.2 Structural Parameter of CuO NPs

The structural parameter for different calcination temperatures at 400 °C, 500 °C, and 600 °C is shown in Table 2. The maximum crystallite size, $D(\text{nm})$ was 30.77 nm at 400 °C and the minimum crystallite size, $D(\text{nm})$ was 13.25 nm at 500 °C. The maximum dislocation density, $\delta(\text{line}/\text{nm}^2 \times 10^{-3})$ was 5.70 at 500 °C and the minimum dislocation density, $\delta(\text{line}/\text{nm}^2 \times 10^{-3})$ was 1.06 at 400 °C. The maximum microstrain, $\mathcal{E}(\times 10^{-3})$ was 1.34 at 500 °C and the minimum microstrain, $\mathcal{E}(\times 10^{-3})$ was 0.85 at 400 °C.

It is shown (in Fig. 4) that the average crystallite size decreases from 400 °C to 500 °C with increasing calcination temperature and then increases with temperature. It is shown (in Fig. 5) that the dislocation density increases with increasing calcination temperature up to 500 °C and then decreases with temperature.

Table 2 Structural parameter for different calcination temperatures

Temperature(°C)	Crystallite Size, $D(\text{nm})$	Dislocation density, $\delta(\text{line}/\text{nm}^2 \times 10^{-3})$	Microstrain, $\mathcal{E}(\times 10^{-3})$
400	30.77	1.06	0.85
500	13.25	5.70	1.34
600	21.78	2.11	1.18

Fig. 4 Calcination temperature versus crystallites size

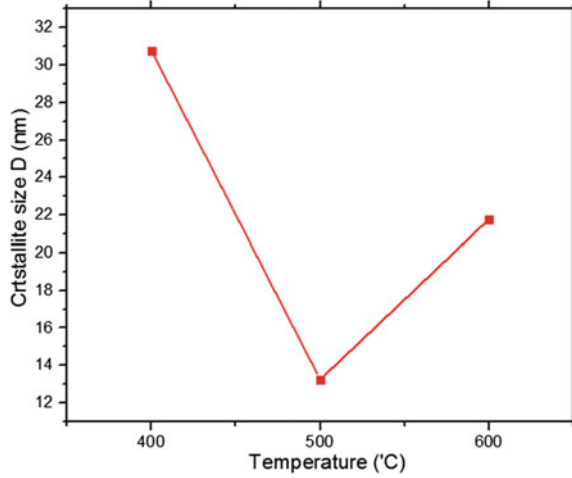
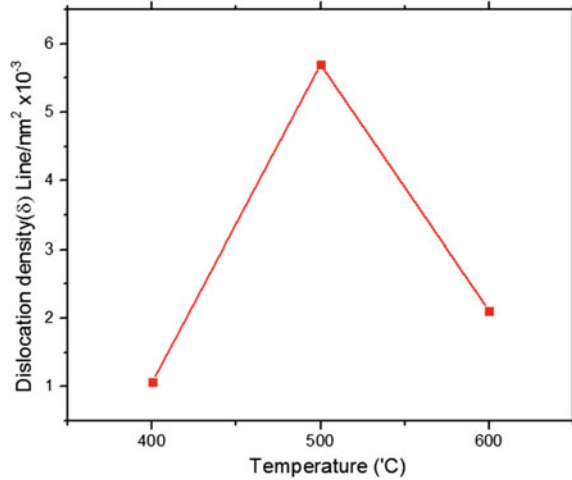


Fig. 5 Calcination temperature versus Dislocation density (δ)



3.3 Williamson–Hall Method

Williamson–Hall X-ray line broadening analysis provides a method of finding an average size of coherently diffracting domains and strain. Strain-induced peak broadening arises due to crystal imperfection; and distortion, which had been calculated using the relation :

$$\epsilon = \frac{\beta}{4\tan\theta} \tag{1}$$

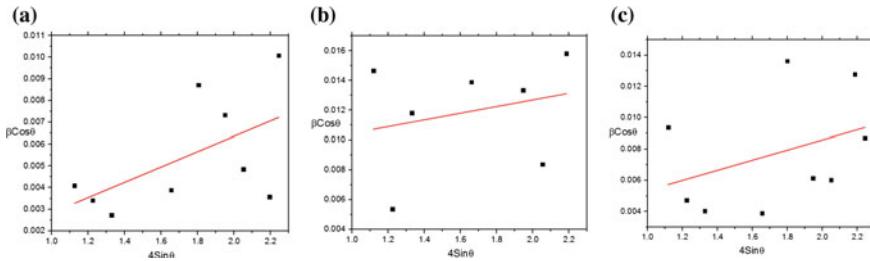


Fig. 6 Slope of the plots provides the value of strain. The slope for 400°C, 500°C, and 600°C are 3.53×10^{-3} , 2.24×10^{-3} , and 3.23×10^{-3} , respectively

To estimate microstrain from the X-ray diffraction pattern, Williamson and Hall [9] proposed a modified Scherrer's formula as follows:

$$\beta \cos \theta = \frac{k\lambda}{D} + 4\epsilon \sin \theta \quad (2)$$

The equation represents the linear plot of $\beta hkl \cos \theta$ against $4 \sin \theta$ for the samples calcined at (a) 400 °C, (b) 500 °C, and (c) 600 °C temperatures displayed in Fig. 6. The slope of the plots provides the values of strain (ϵ) [9].

It is shown (in Fig. 6) that the plots provide the value of the strain, which varies with temperatures. The value of the slope of the strain was 3.53×10^{-3} , 2.24×10^{-3} , and 3.23×10^{-3} at 400°C, 500°C, and 600°C, respectively. It is found that the maximum value of the slope of the strain was 3.53×10^{-3} at 400 °C and the minimum value of the slope of the strain was 2.24×10^{-3} at 500 °C.

3.4 Surface Morphology Analysis: SEM and FESEM

The SEM images of CuO NPs calcined at 400 °C and 500 °C are shown in Fig. 7a and Fig. 7b. The SEM image shows that the samples are in the nano range. The FESEM

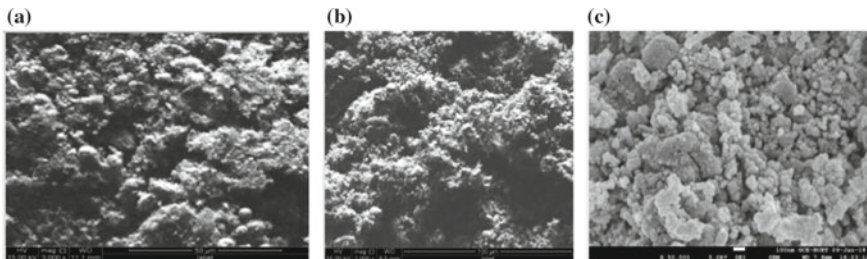


Fig. 7 Surface morphology analysis using SEM and FESEM

image of CuO Nanoparticles (NPs) calcined at 600 °C is shown in Fig. 7c. The image shows that the surface morphology of the Nanoparticles (NPs) is homogeneous and almost spherical in shape.

3.5 Functional Group Analysis of Nanoparticles Using FTIR Technique

Table 3 shows the functional group analysis of Nanoparticles (NPs) using the FTIR technique. It is also found from Table 3 that the maximum peak position(cm^{-1}) of the functional group was 3460 for (-OH) and the minimum peak position(cm^{-1}) of the functional group was 515 for (Cu-O).

It is shown (in Fig. 8) that the stretching vibration of -OH functional group is at the peak position of 3460 cm^{-1} . Whereas, the antisymmetric stretching vibration of -CH₂- is in naphthalic or aliphatic at the peak position of 2925 cm^{-1} . Again, it is also shown that the stretching vibration of -OH functional group is in polyols at the

Table 3 Table for FTIR analysis of CuO NPs

Functional Group	Peak Position(cm^{-1})	Attribution
- OH	3460	Stretching vibration of -OH functional Group
- CH ₂ -	2925	Antisymmetric stretching vibration of -CH ₂ - in naphthalic or aliphatic
- OH	1416	Stretching vibration of -OH in polyols
C-N	1050	Stretching vibration of C-N in amines
Cu-O	515	Stretching vibration of Cu-O bond

Fig. 8 FTIR analysis of CuO NPs

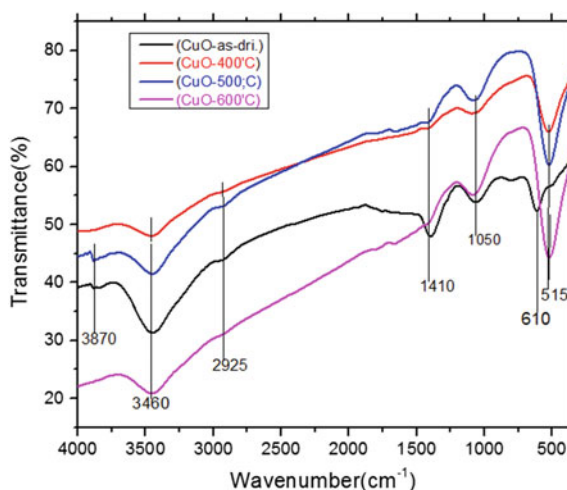
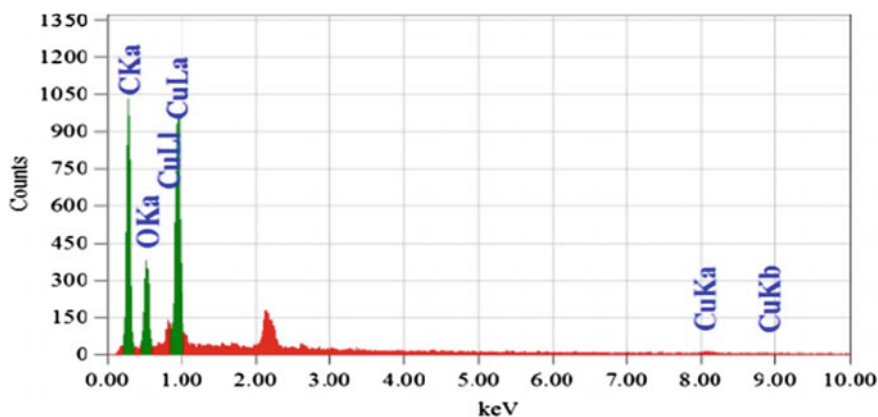


Table 4 Elemental analysis

Elements	Mass (%)
Copper (Cu)	40.36
Oxygen (O)	20.52
Carbon (C)	39.12

**Fig. 9** Elemental analysis of CuO NPs calcined at 600 °C using EDX

peak position of 1416 cm^{-1} , whereas, the stretching vibration of C-N is in amines at the peak position of 1050 cm^{-1} . Finally, it is shown that the stretching vibration of Cu-O bond is at the peak position of 515 cm^{-1} .

3.6 Elemental Analysis of CuO NPs

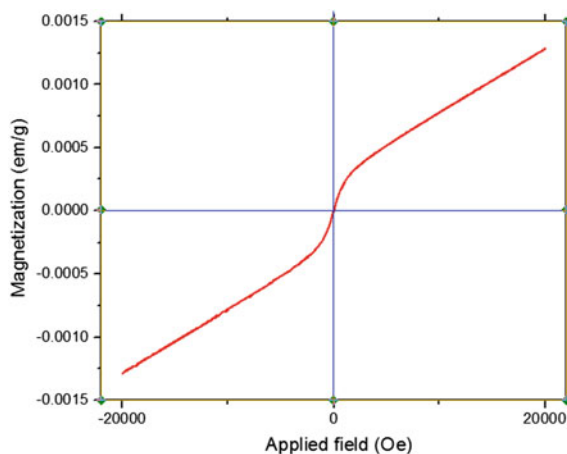
Table 4 shows the Elemental Analysis of CuO Nanoparticles (NPs). It is shown that the mass (%) of Copper (Cu), Oxygen (O), and Carbon (C) are 40.36%, 20.52%, and 39.12%, respectively.

It can be seen that (from Fig. 9) no coercivity or remanence could be observed for the sample, suggesting the diamagnetic properties of the magnetite nanoparticles. This can be ascribed to the small size of nanoparticles which were smaller than the diamagnetic critical size.

3.7 Elemental Analysis and Magnetization of CuO NPs

It is shown (in Fig. 10) that the saturation magnetization of the nanoparticles (NPs) was 0.00125 emu/g .

Fig. 10 Magnetization measurement: VSM image of CuO NPs



3.8 Thermal Analysis of Nanoparticles Using TGA

In the TGA plot (from Fig. 11), the total weight losses are observed 13.33% up to 1100 °C. The weight losses are observed 2.36% up to 700 °C and 10.81% up to 800–1000 °C flat line stabilizes the pure CuO NPs with no impurities.

Fig. 11 TGA plot of CuO NPs calcined at 600 °C

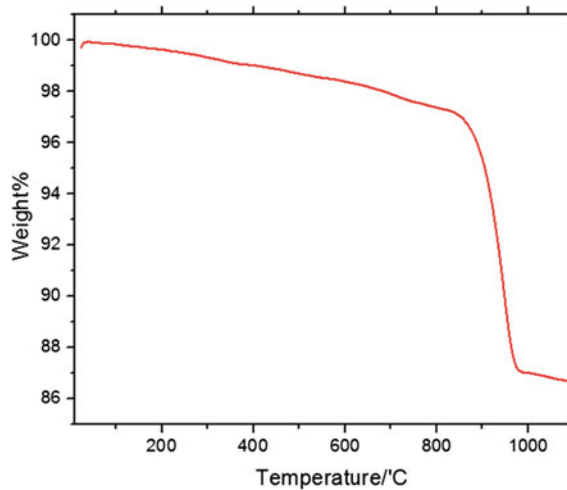
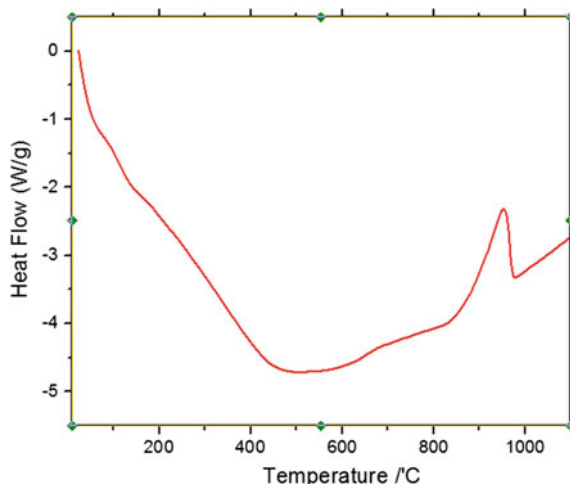


Fig. 12 DSC plot of CuO NPs calcined at 600 °C



3.9 Thermal Analysis of Nanoparticles Using DSC

The DSC curve shows (from Fig. 12) a broad exothermic dip in between room temperature and 500 °C. There is also a sharp dip observed at around 950 °C, which might be due to crystallization and condensation to the anatase phase.

4 Conclusions

The XRD pattern of the average crystallite size was estimated for the synthesized spherical monocyclic crystalline typed CuO NPs as 21.96 nm. NPs synthesized with various calcination temperature also confirmed their crystallinity by XRD analysis and it was found that all of them have pure crystal phase with a spherical monocyclic crystalline structure, where the crystallites size of the NPs decreased with the increase of calcination temperature 400 to 500 °C and crystallite size increases with 600 °C. EDX spectra confirmed the presence of elemental components of the CuO NPs. FTIR spectroscopy showed the involvement of biomolecules present in the extract of *Cathranthus roseus*, which were verified in the synthesizing process of CuO NPs. The formation of CuO NPs was confirmed due to the noticeable absorption peaks at 520 cm^{-1} . The FESEM image showed the high degree of crystallinity of the synthesized CuO NPs in which surface morphology was found to be homogeneous and almost spherical in shape with the presence of capping agents that stabilize the CuO NPs. The thermal analyses were carried out using DSC and TGA techniques in which the synthesized CuO NPs were responded with temperature. The magnetic properties of prepared CuO NPs are examined by VSM which demonstrates that the

synthesized CuO NPs showed slightly superparamagnetic characteristics with zero corrosivity and remanence magnetization property.

Acknowledgements The authors are grateful to the GARE (Grant of Advanced Research in Education) project, Ministry of Education, GoB for financing during the research work (Project/User ID: PS2019949).

References

1. Dr. Khan, M.K.A.: An Introduction to Solar Energy. Mizan Library, Dhaka, Bangladesh (2006)
2. Rai, G.D.: Solar Energy Utilization. Khanna Publishers, Delhi-110006, India (2004)
3. Gunawan, et al.: Energy storage system from galvanic cell using electrolyte from a plant as an alternative renewable energy. IOP Conf. Ser.: Mater. Sci. Eng. **509**, 012045 (2019)
4. Hamid, M.R.: Characterization of a battery cell fueled by bryophyllum pinnatum sap. Int. J. Sci. Eng. Res. **4**(3), 1–4 (2013). ISSN 2229-5518
5. Hamid, M.R., Yusuf, A., Wadud, A.M.A., Rahaman, M.M.: Design and performance test of a prototype of a 12 Volt DC battery fueled by bryophyllum pinnatum sap and improvement of its characteristics, department of electrical and electronic engineering, Ahsanullah university of science and technology, Dhaka, Bangladesh. Int. J. Electron. Electr. Eng. **4**(5), 398–402 (2016)
6. Elgammal, A., Sharaf, A.M.: Dynamic self adjusting FACTS-switched filter compensation, schemes for wind-smart grid interface systems Int. J. Renew. Energy Res. **2**(1), 103–111 (2016)
7. Nedaei, M.: Wind energy potential assessment in Chalus county in Iran. Int. J. Renew. Energy Res. **2**(2), 338–347 (2012)
8. Tzen, E., Papapetrou, M.: Promotion of renewable energy sources for water production through desalination. Desalination Water Treat. **39**(1–3), 302–307 (2012)
9. Ying, C.Y., Dayou, J.: Modelling of the electricity generation from living plants. J. Teknol. **78**(6), 29–33 (2016)
10. Chee, F.P., Chen, C.A., Chang, J.H.W., Choo, Y.Y., Dayou, J.: Data acquisition system for in situ monitoring of chemolectrical potential in living plant fuel cells. J. Biophys. (2016)
11. Volkov, A.G., Foster, J.C., Jovanov, E., Markin, V.S.: Anisotropy and nonlinear properties of electrochemical circuits in leaves of Aloe vera L. Bioelectrochem. **81**(1), 4–9 (2011)
12. Choo, Y.Y., Dayou, J., Surugau, N.: Origin of weak electrical energy production from living-plants Int. J. Renew. Energy Res. **4**(1), 198–203 (2014)
13. Ghate, N.B., Hazra, B., Sarkar, R., Mandal, N.: vitro anticancer activity of Spondias pinnata bark on human lung and breast carcinoma. Cytotechnology **66**(2), 209–218 (2014)
14. Kamal, S., Akhter, R., Tithi, N.A., Wadud, M.A., Narjish, S.N., Shahriar, M., Bhuiyan, M.A.: Biological investigations of the leaf extract of Spondias pinnata. Int. J. Pharm. Sci. Rev. Res. **6**(8), 3351 (2015)
15. Bogdanski, S., Ashton, A., Fogg, A., Burns, D.T., Headridge, J., Sowerbutts, A., East, G., Bishop, E., Bark, L., Grime, J.: Research topics in analytical chemistry. Proc. Soc. Anal. Chem. **9**(9), 182–211 (1972)
16. Lau, O.W., Luk, S.F.: A survey on the composition of mineral water and identification of natural mineral water. Int. J. Food Sci. Technol. **37**(3), 309–317 (2002)
17. Khan, M.K.A., Paul, S., Rahman, M.S., Kundu, R.K., Hasan, M.M., Moniruzzaman, M., Mamun, M.A.: A study of performance analysis of PKL electricity generation parameters: (An experimental analysis on voltage regulation, capacity and energy efficiency of pathorkuchi leaf (PKL) electricity cell). In: Power India International Conference (PIICON), 2016 IEEE 7th, 2016, pp. 1–6. IEEE (2016)

18. Khan, M.K.A., Rahman, M.S., Das, T., Ahmed, M.N., Saha, K.N., Paul, S.: Investigation on parameters performance of Zn/Cu electrodes of PKL, AVL, tomato and lemon juice based electrochemical cells: a comparative study. In: Electrical Information and Communication Technology (EICT), 2015 3rd International Conference on, pp. 1–6. IEEE (2017)
19. Khan, K.A., Rahman, A., Rahman, M.S., Tahsin, A., Jubyer, K.M.: Paul, S.: Performance analysis of electrical parameters of PKL electricity (An experimental analysis on discharge rates, capacity & discharge time, pulse performance and cycle life & deep discharge of Pathor Kuchi Leaf (PKL) electricity cell). In: Innovative Smart Grid Technologies-Asia (ISGT-Asia), 2016 IEEE, pp. 540–544. IEEE (2016)
20. Khan, M.K.A., Paul, S., Rahman, M.S., Kundu, R.K., Hasan, M.M., Moniruzzaman, M., Al Mamun, M.: A study of performance analysis of PKL electricity generation parameters: (An experimental analysis on voltage regulation, capacity and energy efficiency of pathor kuchi leaf (PKL) electricity cell). In: Power India International Conference (PIICON), 2016 IEEE 7th, pp. 1–6. IEEE (2016)
21. Paul, S., Khan, K.A., Islam, K.A., Reza, M.A.: Modeling of a Biomass Energy based (BPL) Generating Power Plant and its features in comparison with other generating Plants. IPCBEE **44** (2012). IACSIT Press, Singapore. <https://doi.org/10.7763/PCBEE.2012.V44.3>
22. Khan, K.A., Paul, S.: A analytical study on electrochemistry for PKL (Pathor Kuchi Leaf) electricity generation system. In: Publication date 2013/5/21, Conference- Energytech, 2013 IEEE, pp. 1–6. Publisher, IEEE (2013)
23. Hasan, M., Khan, K.A.: *Bryophyllum pinnatum* leaf fueled cell: an alternate way of supplying electricity at the off-grid areas in Bangladesh. In: Proceedings of 4th International Conference on the Developments in Renewable Energy Technology [ICDRET 2016], p. 01, (2016). <https://doi.org/10.1109/ICDRET.7421522>
24. Hasan, M., Khan, K.A., Mamun, M.A.: An estimation of the extractable electrical energy from bryophyllum pinnatum leaf. Am. Int. J. Res. Sci-Ence, Technol. Eng. Math. (AIJRSTEM) **01**(19), 100–106 (2017)
25. Khan, M.K.A., Rahman, M.S., Das, T., Ahmed, M.N., Saha, K.N., Paul, S.: Investigation on parameters performance of Zn/Cu electrodes of PKL, AVL, tomato and lemon juice based electrochemical cells: a comparative study. In: Electrical Information and Communication Technology (EICT), 2017 3rd International Conference on, pp. 1–6. IEEE (2017). <https://doi.org/10.1109/EICT.2017.8275150>, IEEE, Khulna, Bangladesh, Bangladesh, 7–9
26. Duffie, J.A., Beckman, W.A.: Solar Energy Thermal Process. John Wiley and Sons. Inc N.Y. USA
27. Sharma, B.K.: (1998) Electrochemistry, Krishna Prakashan Media (P) Ltd., 11, Shivaji Road, Meerut-250 001 (UP) India (1998)